Submonolayer growth of H_2-phthalocyanine on Ag(111)

Ingo Kröger,[1,2,*] Patrick Bayersdorfer,[3,4] Benjamin Stadtmüller,[1,2] Christoph Kleimann,[1,2] Giuseppe Mercurio,[1,2] Friedrich Reinert,[3,4] and Christian Kumpf[1,2]

[1]*Peter Grünberg Institut (PGI-3), Forschungszentrum Jülich, 52425 Jülich, Germany*

[2]*Jülich Aachen Research Alliance (JARA)-Fundamentals of Future Information Technology, 52425 Jülich, Germany*

[3]*Experimentelle Physik 7, Universität Würzburg, Am Hubland, D-97074 Würzburg, Germany*

[4]*Karlsruher Institut für Technologie (KIT), Gemeinschaftslabor für Nanoanalytik, 76021 Karlsruhe, Germany*

(Received 24 August 2012; published 6 November 2012)

We present a comprehensive study of structural and electronic properties of the adsorbate system H_2-phthalocyanine (H_2Pc) on Ag(111). A comparison with copper-phthalocyanine (CuPc) on Ag(111) allows us to elucidate the impact of the central metal atom in the molecule on the adsorbate-substrate interaction. This metal atom is one fundamental parameter which can be changed in order to modify the properties of phthalocyanine molecules, and therefore its influence on the adsorption behavior is highly relevant. From high-resolution electron diffraction, we obtained a phase diagram for submonolayer coverages which turns out to be similar to that of CuPc/Ag(111). The most striking difference is a higher stability of a commensurate phase, indicating a stronger and more adsorption site-specific bonding of the H_2Pc molecules. Furthermore, ultraviolet photoelectron spectroscopy and x-ray standing waves prove chemisorptive interaction between molecules and substrate and a significant bending of the molecules with the nitrogen atoms approaching the surface. We conclude that the attractive interaction of metal-phthalocyanine molecules with Ag(111) is mainly mediated by the aromatic body of the molecule (the tetraazaporphyrin ring in particular) rather than by the central metallic atom which (in the case of CuPc) already shows Pauli repulsion.

DOI: 10.1103/PhysRevB.86.195412 PACS number(s): 68.43.−h, 61.05.jh, 68.49.Uv, 79.60.Dp

I. INTRODUCTION

Interfaces between organic molecules and metal contacts are of special interest in the field of organic electronics since charge injection barriers and thin film morphology have a significant impact on the performance of such organic devices. Currently, phthalocyanine molecules are widely used as absorber and hole transport materials. They are therefore extensively investigated in terms of their electronic properties and growth modes on different substrates.[1–7] The interplay of molecule-substrate and molecule-molecule interactions[8] is of special interest in this context and is generally investigated using well-defined crystalline substrates and well-controlled and reproducible conditions.

In recent studies, we have investigated the adsorption of metal-phthalocyanines such as CuPc (Ref. 9) and SnPc (Refs. 10 and 11) on the Ag(111) surface. The submonolayer growth mode of these molecules is dominated by intermolecular repulsion and weak chemisorptive interaction with the substrate. This leads to a variety of lateral structures, depending on coverage and temperature. In the low-coverage regime, the molecules arrange in a dilute gaslike phase with an average intermolecular distance which continuously decreases with increasing coverage. In this "*g*-phase," no clustering of the molecules into long-range-ordered islands can be observed, even at low temperature (LT, ≈130 K). In the higher-coverage regime and at LT, the formation of a commensurate structure can be observed (CuPc: *c*-phase with one molecule per unit cell; SnPc: c_2-phase with two molecules per unit cell), which originates from the trapping of the densely packed molecules at specific adsorption sites provided by the corrugation of the substrate. Between ≈0.9 and 1.0 ML, the molecules form long-range-ordered superstructures with point-on-line (p.o.l.) coincidence with the substrate. It has been shown that the unit-cell size decreases *continuously* with increasing coverage, which unambiguously proves *repulsive* intermolecular interaction.[9,10] Normal incidence x-ray standing waves (NIXSW) experiments revealing the adsorption heights of the molecules and ultraviolet photoemission spectroscopy (UPS) data of the valence region clearly showed the chemisorptive character of the adsorbate-substrate interaction.[11,12] Subsequent studies of the CuPc adsorption on surfaces with higher and lower reactivity [Cu(111) and Au(111), respectively],[13,14] as well as pair-potential calculations for CuPc on the same surfaces,[15] led to a comprehensive adsorbate model and enabled a good understanding of the delicate interplay of intermolecular forces and the adsorbate-substrate interaction which are responsible for the different adsorption behaviors on different substrates.

In this context, the central metal atom of the phthalocyanine molecule is of special interest because it is believed to play a crucial role in the interaction with the surface. It was suggested that the metal atom significantly contributes to the overlap of electronic states with the substrate[10] and hence strongly influences the exchange of electronic charge between substrate and molecule. A strong molecule substrate interaction, in turn, can influence the intermolecular interaction, as demonstrated for CuPc/Cu(111),[13,15] or increase the "push-back" dipole, if the metal atom of the molecule is strongly involved in form of Pauli repulsion with the substrate.

Here, we report on an investigation of the adsorption of the metal-free H_2Pc on Ag(111) using the same experimental methods as in earlier work on CuPc and SnPc: spot profile analysis low-energy electron diffraction (SPA-LEED), UPS, and NIXSW. The analysis of lateral structures, of (vertical) adsorption heights, and of the electronic structure in the valence-band region for H_2Pc, together with the comparison

 ©2012 American Physical Society

with published data mentioned above, allowed a comprehensive evaluation of the role of the central metal atom in the adsorbate-substrate interaction and structure formation.

II. EXPERIMENT

SPA-LEED and UPS measurements were performed in an ultrahigh vacuum (UHV) system with a base pressure below 5×10^{-10} mbar. The system was equipped with an Omicron SPA-LEED instrument, an Mg K_α x-ray source, a He-discharge lamp for UPS ($h\nu = 21.2$ eV), a hemispherical analyzer ($R = 100$ mm), and adequate equipment for cleaning the substrate crystals (Ag sputtering and annealing) and preparation of the samples [dedicated evaporation sources and quadrupole mass spectrometer (QMS) for monitoring]. The NIXSW experiments were performed at beamline ID32 of the European Synchrotron Radiation Source (ESRF) in Grenoble, France. At the beamline, similar equipment was available, except a conventional LEED optics (instead of the SPA-LEED instrument) and a different hemispherical analyzer ($R = 150$ mm). The latter was mounted with an angle of 45° relative to the incident photon beam.

The Ag(111) surface was prepared by argon sputtering (incident angle: ±50°, $E = 500$ eV) and subsequent annealing at 723 K for 20 min. The H_2Pc molecules, which were purified in two subsequent sublimation procedures beforehand, were evaporated from a dedicated Knudsen cell while monitoring the mass flux with the QMS. The coverage was also determined by x-ray photoemission spectroscopy (XPS) using the integrated C1*s* signal as the relevant measure. The monolayer structure, i.e., that p.o.l. superstructure with the smallest unit-cell size, was used for normalizing the coverage. It can easily be prepared by desorbing a multilayer film at ≈520 K. After deposition, all samples were annealed at 473 K in order to allow diffusion of molecules over step edges and obtain the identical coverage on all surface terraces.

While LEED and XPS/UPS are well-known standard techniques, the NIXSW method shall be briefly introduced here. For more comprehensive introductions, see Refs. 16–19. The method is able to measure the vertical positions (relative to the lattice planes of the substrate crystal) of all atomic species within the molecules with a very high precision of ≈0.05 Å. Adsorption heights and vertical inner geometry (bending and distortions) of adsorbed molecules can thus be obtained.[4,5,9,11,14,20–25] The x-ray standing-wave field is generated by the coherent superposition of an incident ($\vec{E}_0$) and Bragg-reflected ($\vec{E}_H$) wave when the Bragg condition for an $\vec{H} = (hkl)$ reflection is fulfilled: $\vec{H} = \vec{k}_H - \vec{k}_0$. Scanning the photon energy through the Bragg condition leads to a shift of the phase ν of the relative complex field amplitude $E_H/E_0 = \sqrt{R}\,e^{i\nu}$ by π, resulting in a spatial shift of the standing wave by half of the lattice-plane spacing d_{hkl} in the direction perpendicular to the lattice planes. This varies the intensity of the standing-wave field at the positions of each individual atom, which in turn can be probed by measuring the absorption of the atoms via their photoelectron, Auger electron, or fluorescence yield. Here, we use the C1*s* and N1*s* photoelectron yield, corresponding to the energy-integrated XPS signal after proper background subtraction. The result is an element-specific quantity $I(E)$ that can be calculated as follows[16–19]:

$$I(E) = 1 + S_R R + 2|S_I|\sqrt{R}F^H \cos(\nu - 2\pi P^H + \Psi). \quad (1)$$

The essential fitting parameters are the coherent position P^H and the coherent fraction F^H. They represent phase and amplitude, respectively, of the Hth Fourier component of the electron density of the corresponding atomic species. The coherent position can easily be interpreted as the average atomic height D^H, modulo the lattice-plane spacing d_{hkl} of the substrate crystal, and in units of d_{hkl}: $P^H = (D^H \bmod d_{hkl})/d_{hkl}$. Other quantities in Eq. (1), the reflectivity $R(E)$, its complex amplitude $\sqrt{R(E)}$, and the relative phase $\nu(E)$, are derived from fitting the reflectivity curve under consideration of a Gaussian energy broadening due to finite instrumental resolution. The parameters $S_R = (1+Q)/(1-Q)$, $|S_I| = \sqrt{1+Q^2\tan^2\Delta}/(1-Q)$, and $\Psi = \tan^{-1}(Q\tan\Delta)$ contain the multipole correction parameters Q and Δ, which can be found in literature.[16,18,24] The values we used in this work are taken from Ref. 11 and listed in Table I.

TABLE I. Multipole correction parameters for fitting the photoelectron yield curves. Values are taken from Ref. 11.

E		C1s	N1s
2640 eV	Q	0.24	0.22
	Δ	− 0.21	− 0.26

III. RESULTS AND DISCUSSION

A. SPA-LEED results

From SPA-LEED measurements, we obtained the phase diagram shown in Fig. 1. It describes the formation of (lateral) superstructures depending on temperature and coverage. On first view, this phase diagram is very similar to that found for CuPc/Ag(111) (Ref. 9) and SnPc/Ag(111) (Ref. 10). H_2Pc forms a gaslike phase (*g*-phase) in the low-coverage regime in which the molecules lie more or less isolated from each other on the surface. Their average distance decreases continuously with increasing coverage (e.g., 22.5 Å at 0.34 ML, 14.8 Å

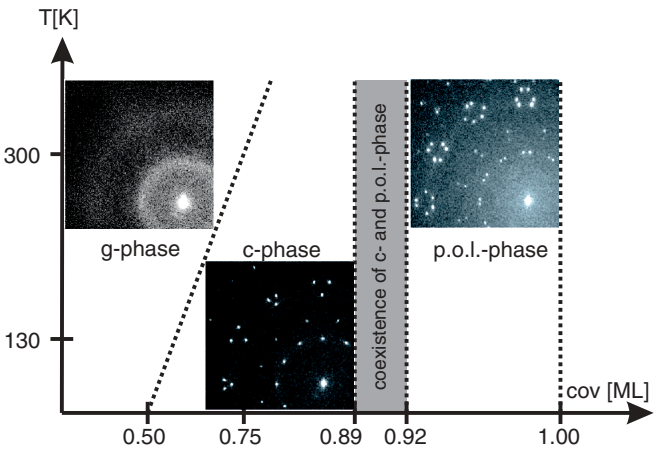

FIG. 1. (Color online) Phase diagram of H_2Pc/Ag(111). The images show exemplary SPA-LEED pattern of the different phases.

at 0.68 ML). In the LEED pattern, this results in a ring of diffuse scattering intensity, as can be seen in Fig. 1, the radius of which continuously increases with increasing coverage. At medium coverages and LT, a commensurate structure is found having the identical unit cell as the *c*-phase of CuPc/Ag(111): the unit-cell matrix is $\left(\begin{smallmatrix}5 & 0\\ 3 & 6\end{smallmatrix}\right)$, with one molecule per unit cell. Note that the SnPc/Ag(111) commensurate structure, the so-called c_2-phase, is different because it has two differently bent molecules in a larger unit cell, one with the Sn atom pointing upwards, one downwards.

Finally, in the high-coverage regime, H_2Pc forms a series of long-range-ordered structures with point-on-line coincidence with the substrate (p.o.l.-phase). Similar to the cases of CuPc and SnPc, the system always maximizes the size of its unit cell in this phase. This leads to a continuous change of the structure when changing the coverage. All unit cells found in the SPA-LEED experiments for this regime are shown in Fig. 2. The circles represent the corners of the unit cells, drawn on the underlying Ag(111) lattice (thin solid lines). The dashed and dotted lines show the smallest and largest unit cells, respectively. Note that the superstructure lattice points are well aligned along lattice lines of the Ag(111) substrate, indicating the point-on-line registry. Numerical values of four exemplary p.o.l. structures are given in Table II. This finding, in particular the *continuous* change of the unit-cell size with changing coverage, demonstrates that intermolecular repulsion is also present for H_2Pc/Ag(111) and not prominently caused by the central metal atom in the systems CuPc/Ag(111) and SnPc/Ag(111).

However, a closer look at the phase diagrams for H_2Pc, CuPc, and SnPc on Ag(111) reveals some significant differences, e.g., the position of the phase boundaries of the commensurate phases (*c*-and c_2-phases). In contrast to CuPc and SnPc/Ag(111), the *c*-phase of H_2Pc is stable at RT, even

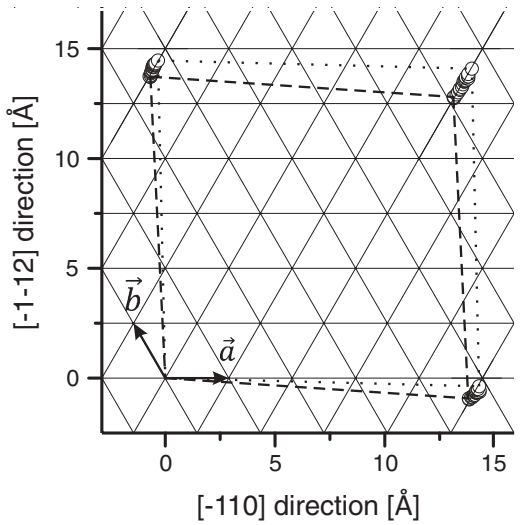

FIG. 2. Unit cells of 20 different p.o.l. structures of H_2Pc/Ag(111). Circles indicate the positions of the corners of the supercells on the Ag(111) lattice (thin solid lines) for different coverages. The smallest (dashed line, coverage 1.00 ML) and largest cell (dotted line, 0.92 ML) are shown. $\vec{a}$ and $\vec{b}$ represent the unit-cell vectors of the Ag(111) substrate lattice.

TABLE II. Epitaxy matrices and unit-cell sizes for the structures occurring at different coverages in the p.o.l.-phase of H_2Pc/Ag(111) derived from SPA-LEED.

Coverage (ML)	Epitaxy matrix	Area (Å^2)
0.93	$\left(\begin{smallmatrix}4.83(4) & -0.25(4)\\ 2.67(4) & 5.71(4)\end{smallmatrix}\right)$	204(3)
0.95	$\left(\begin{smallmatrix}4.73(4) & -0.30(4)\\ 2.60(4) & 5.61(4)\end{smallmatrix}\right)$	198(3)
0.97	$\left(\begin{smallmatrix}4.67(4) & -0.35(4)\\ 2.55(4) & 5.55(4)\end{smallmatrix}\right)$	194(3)
1.00	$\left(\begin{smallmatrix}4.60(4) & -0.37(4)\\ 2.51(4) & 5.49(4)\end{smallmatrix}\right)$	189(3)

in a rather large range of coverages (0.75–0.92 ML). Also at LT the stable range of this structure is extended down to 0.5 ML. Furthermore, a region of coexistence of *c* and p.o.l.-phases was observed at ≈0.9 ML (see Fig. 1). This has been found in SPA-LEED by reducing the coverage from 1.00 ML to ≈0.9 ML (by desorbing molecules at $T \geqslant 523$ K). During annealing, the LEED spots stemming from the p.o.l.-phase continuously change their position in the LEED image, indicating the continuous change of the unit cell which is characteristic in this regime. When the coverage falls below ≈0.91 ML, additional diffraction spots of the *c*-phase appear. The situation is illustrated in the SPA-LEED images shown in Fig. 3, where green and red circles mark the LEED spots from p.o.l.-and *c*-phases, respectively. This indicates a phase separation in this rather narrow coverage regime and a coexistence of *c*-phase and p.o.l-phase domains, which was not found for CuPc or SnPc/Ag(111).

Summarizing the SPA-LEED measurements, we can state that, compared to CuPc/Ag(111), the *c*-phase of H_2Pc/Ag(111) exists in an extended region of both coverage and temperature, and hence is more stable. This allows us to conclude a stronger and possibly more local character for the H_2Pc-substrate interaction. This can be caused by a higher site specificity of the molecule-substrate bonding and/or by an additional or stronger short-range intermolecular attraction.

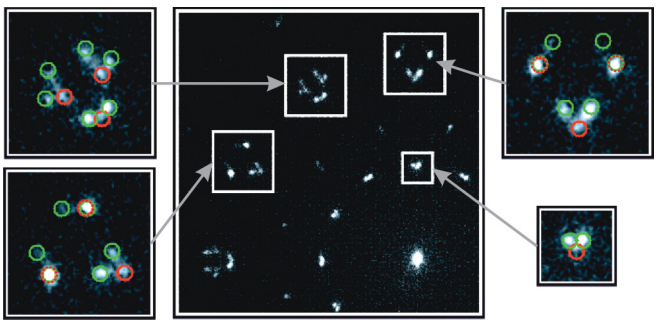

FIG. 3. (Color online) SPA-LEED pattern for a coverage of ≈0.91 ML H_2Pc/Ag(111), i.e., within the coexistence regime of *c* and p.o.l.-phases. In the enlarged insets, calculated peak positions for both phases are shown in red and green for the *c* and p.o.l.-phases, respectively. The corresponding unit-cell matrices are $\left(\begin{smallmatrix}5 & 0\\ 3 & 6\end{smallmatrix}\right)$ (red) and $\left(\begin{smallmatrix}4.86 & -0.16\\ 2.74 & 5.72\end{smallmatrix}\right)$ (green).

B. UPS investigations

In a recent comparative UPS study of cobalt-tetraphenylporphyrine (Co-TTP) and H_2-TTP, Gottfried *et al.* reported the occurrence of two resonances, which clearly are induced by the Co atom.[6,26,27] The observed features are located close to the Fermi edge in the CoTTP/Ag(111) spectra, but not visible in the H_2-TTP data. The authors concluded a coordination of the Co ion with the substrate as the reason for these features. The electronic valence states were also visible in STM measurements, in the form of a much higher tunneling current in the center of the Co-TTP molecules compared to the H_2-TTP molecules. For metal-phthalocyanines, a similar situation was found: Also here a much more distinct STM contrast is visible in the center of the metal-Pc molecule as compared to H_2Pc.[7,28,29] This made us perform a similar UPS investigation for CuPc and H_2Pc on Ag(111), the results of which are presented in Fig. 4. Spectra of both systems, recorded at a coverage of 0.7 ML at RT, i.e., in the regime of the *g*-phase, are shown. Experimental conditions were identical for both measurements at a resolution of ≈100 meV, an emission angle of 45°, and identical preparation conditions. All spectra were normalized to the count rate at the binding energy $E_{\mathrm{Bin}} = 0.6$ eV. Note that, apart from small shifts in binding energy,[9] the spectral features do not depend on coverage.

The valence band of CuPc/Ag(111) is dominated by four spectral features: the highest and second highest occupied molecular orbitals (HOMO and HOMO-1), the (former) lowest unoccupied molecular orbital (F-LUMO), which became partly filled due to the interaction between molecule and substrate including exchange of electronic charge between molecules and substrate,[9,10] and a split-off (SO) state which is discussed in more detail in Ref. 9 where data with better energy resolution are shown. The valence band of H_2Pc/Ag(111), in contrast, only shows two features, the F-LUMO and the HOMO. HOMO-1 and the SO state are missing in this binding-energy regime. This is illustrated by the difference spectrum, where HOMO and F-LUMO cancel out very well, and HOMO-1 and the SO state remain. The remaining small feature in the region of the HOMO originates from slightly different binding energies and linewidths of the HOMO states of both molecules.

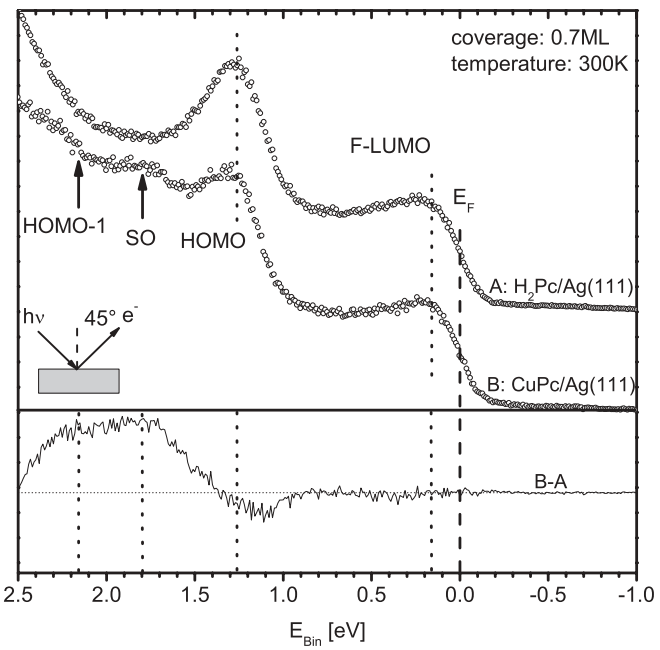

FIG. 4. Comparison of UPS data of 0.7 ML of CuPc (curve A) and H_2Pc (curve B) on Ag(111). Both spectra were normalized to the count rate at $E_{\mathrm{Bin}} = 0.6$ eV. In the bottom, the difference spectrum B−A is shown.

This finding allows the conclusion that the F-LUMO and HOMO orbitals of CuPc have no major contribution from the copper atom since they are identical to those of H_2Pc. The SO state, however, originates from the interaction of the coordinated Cu ion with the substrate, as well as the HOMO-1 regarding its energetic position. This is in good agreement with results obtained earlier for the physisorbed CuPc on the Au(111) surface,[13,14] where HOMO-1 and the SO state are also not observed. We can therefore conclude that the charge transfer from the substrate to the molecule, which is visible in the F-LUMO resonance, is (on a quantitative level) identical for CuPc and H_2Pc/Ag(111). This so-called back-donation of charge, which is characteristic for the adsorbate-substrate interaction, is hence localized at the aromatic body of the molecules, i.e., on the tetraazaporphyrin ring containing the nitrogen atoms. If this is correct, also the adsorption heights of both molecules should be very similar, a question which will be answered in the NIXSW study reported in the following.

C. NIXSW investigations

We have investigated three different coverages of H_2Pc/Ag(111), each at 300 K (RT) and 183 K (LT), with NIXSW: 0.7 ML and 0.8 ML, both representing the commensurate phase, and 0.93 ML, which is located in the p.o.l. regime. The partial photoelectron yield was obtained from N1*s* and C1*s* spectra by correcting for background and integrating (see Fig. 5). For the C1*s* spectra we used a linear background, which was chosen such that the C1*s* satellites in the binding-energy range between 298 and 292 eV were excluded since we observed artifacts caused by the electron analyzer in this region. The same effect occurred in the data published in Ref. 14, and was proven not to compromise the results. For the N1*s* spectra, the background function consists of a linear component and three Gaussians representing plasmon satellites from the Ag3*d* lines. This fitting model has also been used earlier.[9–11,13]

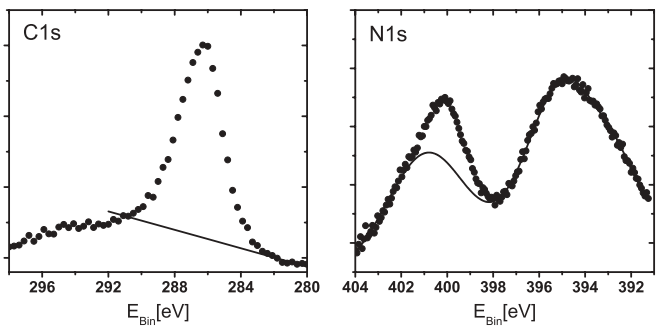

FIG. 5. Exemplary XPS spectra (circles) and subtracted background functions (lines) of the C1*s* and N1*s* core levels of H_2Pc/Ag(111).

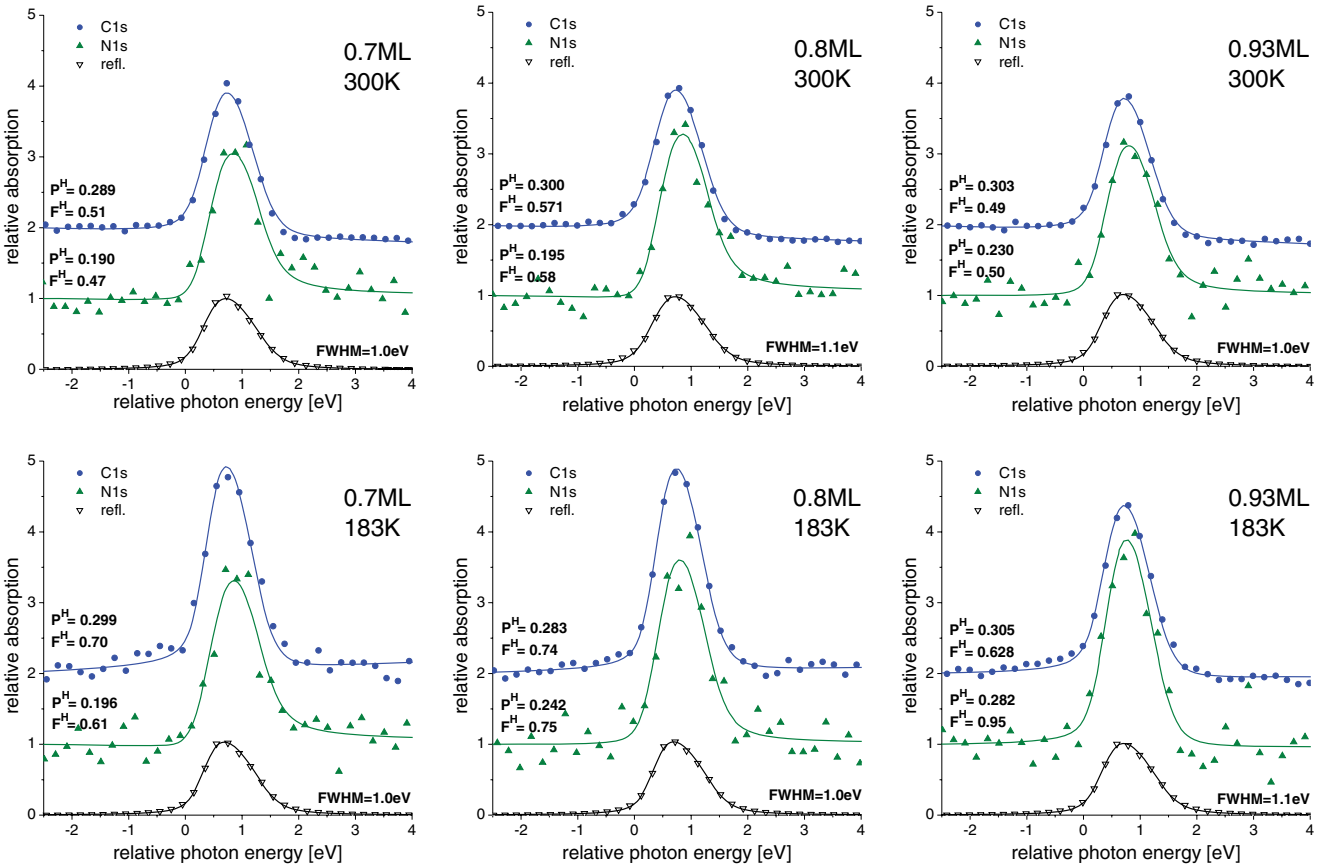

FIG. 6. (Color online) NIXSW photoelectron yield and reflectivity curves of H_2Pc/Ag(111) structures at different coverages and temperatures. Experimental data were fitted using Eq. (1).

Beam damage caused by the x-ray synchrotron beam or impinging electrons is a crucial issue for the investigation of organic thin films. In the case of NIXSW, beam damage causes a decrease of the coherent fraction of the adsorbate species[30] because the relevant order of the system (in our case, the uniformity of the adsorption height) is reduced by molecules which were destroyed by the x-ray beam. For H_2Pc, this effect was found to be significantly stronger than for the metal-Pc molecules. Already after exposure times of 10 min, we could detect the first indications of radiation damage. Hence, we adjusted the duration of one NIXSW scan such that the exposure time of each spot on the sample did not exceed 8 min. This was only possible with a very short integration time in the individual XPS spectra and caused a rather poor signal-to-noise ratio, which had to be compensated by repeating the measurement on many different spots on the sample. Summing up these data finally gave a good quality for the NIXSW yield curves, which could easily be further analyzed. However, fitting of individual NIXSW scans from only one spot was not possible. Consequently, the uncertainties of the fitting parameters could not be obtained from the statistics of the individual fitting results, as we have done earlier.[9–11,13] Therefore, the results shown here always correspond to summed yield curves, and errors were estimated based on the experience of earlier NIXSW measurements.[9,14] Note that the C1*s* yield curves show a weak linear slope that can originate from the shortened background subtraction in the XPS spectra. Another possible reason would be a drifting beam position on the sample caused by scanning the photon energy. In any case, we considered this effect by an additional linear term in the fit function.

Our NIXSW results for all six data sets mentioned above are shown in Fig. 6. Each panel contains yield curves for N1*s* and C1*s*, fitted using Eq. (1), and the corresponding x-ray reflectivity curve. The results are given in terms of P^H and F^H in the figure, and illustrated in Fig. 7 as a true-scale model. The circles with solid lines denote the covalent bond radii of the individual atoms,[31] and dotted circles correspond to nonbonding van der Waals radii.[32]

It can be seen immediately, that all adsorption heights D^H are smaller than the sum of the corresponding van der Waals radii (C-Ag: 3.49 Å, N-Ag: 3.27 Å), which indicates the chemisorptive bonding character. This is in good agreement with a significant overlap of molecular wave functions and substrate states and the consequent exchange of electronic charge found in the UPS results discussed above. We further note that the adsorption heights for the carbon atoms are very similar to those found for CuPc/Ag(111).[9] The nitrogen atoms of H_2Pc located in the tetraazaporphyrin ring, however, are found significantly closer to the substrate ($D_C^H - D_N^H \approx 0.26$ Å). This indicates a bending of the molecule, which was not observed for CuPc/Ag(111). The magnitude is comparable to the bending of 3,4,9,10-perylene-tetracarboxylicacid-dianhydride (PTCDA) and 1,4,5,8-naphthalene-tetracarboxylicacid-dianhydride (NTCDA) on Ag(111).[4,20,22,24,33] It should also be mentioned that the

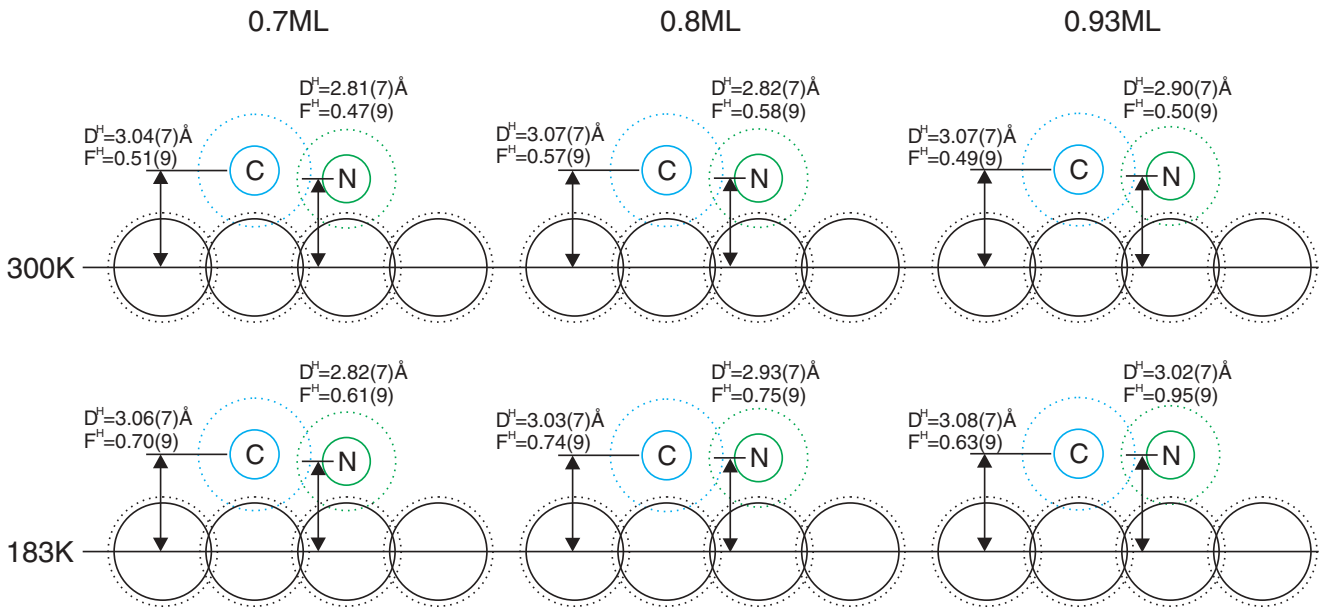

FIG. 7. (Color online) Real-scale model of the adsorption heights of the investigated structures of H_2Pc/Ag(111). Full circles indicate covalent bonding radii (Ref. 31) and dotted circles van der Waals radii (Ref. 32).

adsorption heights change with coverage. Very similar to the case of CuPc/Ag(111), the molecule lifts up by ≈0.2 Å when the coverage increases. The bonding of the molecules is weakened by the next-neighbor molecules getting closer since the molecules are competing with each other for the charge transfer to the substrate. The effect is discussed in detail in Ref. 9.

Hence, H_2Pc/Ag(111) adsorbs in an "N-down" geometry. The small N-Ag distance could be misunderstood as a proof for a strong N-dominated bonding of the H_2Pc, stronger than in the case of CuPc. The UPS data shown in Fig. 4 are not consistent with such an interpretation since they show very similar valence-band spectra and in particular a similar filling of the F-LUMO state for both systems. Hence, adsorption heights have to be discussed in a different perspective, they need to be set in relation with bonding (covalent) or nonbonding (van der Waals) radii, i.e., the different size of the atoms involved must be considered (see also Refs. 14 and 33). Since both covalent and van der Waals radii scale in a similar manner, it is not crucial which radii are taken as reference. Since the distances measured here are closer to van der Waals radii, we select those for a normalization of the adsorption heights obtained from the NIXSW analysis.

In Table III, the bonding distances for C, N, and Cu are listed for H_2Pc/Ag(111) and CuPc/Ag(111) in relative units of the sum of the relevant van der Waals radii, e.g., $d_C = D_C^H / (r_C^{vdW} + r_{Ag}^{vdW})$. For comparison, we also list the covalent bonding distances of C-Ag, N-Ag, and Cu-Ag in units of the van der Waals radii (last line of the table). These values indicate the lower limit of the relative adsorption heights which correspond to a purely covalent bond between the atoms involved. The higher limit of course is 1.0, complying with physisorption.

Note that all these relative bonding distances are significantly smaller than 1.0. With respect to the possible range of 0.63 . . . 1.0 (C-Ag), 0.66 . . . 1.0 (N-Ag), and 0.89 . . . 1.0 (Cu-Ag), all values are roughly 2/3 on the way from a chemical bond length to van der Waals distance. This indicates weak chemisorption. A closer look on the numbers for nitrogen and carbon makes clear that the situation for these two species is actually quite comparable in terms of bonding distances (all values are between 0.86 and 0.90, with only one exception). For CuPc, the situation is different. Here, the values for nitrogen (0.90...0.94, also those for copper 0.93...0.97) are significantly larger than those for carbon (≈0.87). This indicates that for CuPc, an N-down configuration, as it was found for H_2Pc, might be inhibited by the N-Cu coordination and the Pauli repulsion between the copper atom and the

TABLE III. Adsorption heights of C, N, and Cu atoms in H_2Pc/Ag(111) and CuPc/Ag(111), normalized to the corresponding sum of van der Waals radii. Values for CuPc are taken from Ref. 9, van der Waals radii from Ref. 32: $r_C^{vdW} = 1.77$ Å, $r_N^{vdW} = 1.55$ Å, $r_{Cu}^{vdW} = 1.40$ Å, and $r_{Ag}^{vdW} = 1.72$ Å. For comparison, we list covalent bonding distances of C, N, and Cu to Ag in the last line, also in units of the van der Waals radii. Covalent bonding radii are taken from Ref. 31: $r_C^{cov} = 0.76$ Å, $r_N^{cov} = 0.71$ Å, $r_{Cu}^{cov} = 1.32$ Å, and $r_{Ag}^{cov} = 1.45$ Å.

	T (K)	cov (ML)	d_C	d_N	d_{Cu}
H_2Pc	300	0.93	0.88(2)	0.89(2)	
	300	0.8	0.88(2)	0.86(2)	
	300	0.7	0.87(2)	0.86(2)	
H_2Pc	183	0.93	0.88(2)	0.92(2)	
	183	0.8	0.87(2)	0.90(2)	
	183	0.7	0.88(2)	0.86(2)	
CuPc	300	1.0	0.88(1)	0.93(1)	0.95(1)
	300	0.85	0.86(1)	0.93(1)	0.93(1)
	300	0.5	0.87(1)	0.92(1)	0.96(1)
CuPc	153	1.0	0.88(1)	0.94(1)	0.97(1)
	140	0.85	0.86(1)	0.92(1)	0.94(1)
	140	0.5	0.86(1)	0.90(1)	0.93(1)
Covalent bonding distances			0.63	0.66	0.89

substrate. HOMO-1 and SO states in the UPS data (Fig. 4), which have been identified as Cu-induced states, clearly indicate the interaction of the copper atom with the substrate. Similar to the case of Co-TPP, they can be interpreted as the bonding and antibonding states of an Ag-Cu hybrid orbital.[26,27] Since both states are fully occupied and located far below the Fermi energy, they can not significantly contribute to the bonding of the molecule to the substrate, as it is the case for the F-LUMO. For this reason, the Cu atom (and, in general, the metal atom of other metal-Pcs) has only little influence on the bonding strength of these molecules.

Furthermore, the coordination of the nitrogen atoms to the central copper atom is expected to reduce their reactivity. It is known that the nitrogen atoms in the H_2Pc molecule are quite reactive. Metalation reactions of H_2Pc and H_2-TPP have been reported frequently upon coadsorption of metal atoms such as Fe, Ni, and Zn.[6,26,34,35] Obviously, the metalation reactions also depend on the reactivity of the metal atom since silver adatoms, which are certainly present at RT at the Ag(111) surface, were not found to incorporate into the H_2Pc or H_2-TPP molecules. Therefore, we can conclude that the N-down configuration of H_2Pc on Ag(111) is a result of a weak but very site-specific bonding of the nitrogen atoms to the Ag(111) surface. This site specificity leads to the higher stability of the commensurate phase at room temperature and at lower coverages as observed in SPA-LEED measurements.

IV. SUMMARY

In this study, we compared the lateral structures, adsorption heights, and valence-band spectra of H_2Pc/Ag(111) and CuPc/Ag(111) in order to investigate the role of the central copper atom in the adsorption process. From UPS, we could conclude that the HOMO-1 and SO states of the CuPc originate from the interaction of the copper atom with the substrate, while the HOMO and F-LUMO are mainly localized at the aromatic tetraazaporphyrin ring of the molecule, as it is also the case for H_2Pc/Ag(111). NIXSW measurements show a strong N-down configuration for H_2Pc molecules, which was not observed for CuPc/Ag(111). The comparison of the *relative* adsorption heights indicates that this N-down configuration leads to similar bonding distances of carbon and nitrogen to the substrate atoms. The copper atom in the CuPc molecule prevents this configuration due to its coordination with the nitrogen atoms and due to Pauli repulsion with the substrate. Furthermore, the N-down configuration of H_2Pc/Ag(111) leads to a more adsorption site-specific bonding to the substrate and hence to the higher stability of the commensurate phase. In agreement with SPA-LEED measurements, this allows the conclusion that the central metal atom of metal-Pc molecules on Ag(111) has no crucial impact on either the adorbate-substrate interaction or the intermolecular repulsion observed in these adsorbate systems.

ACKNOWLEDGMENTS

We would like to thank Y. Mi, P. Rajput, and J. Zegenhagen for their support during the NIXSW beam time, and M. Gottfried, M. Häming, and J. Ziroff for stimulating discussions. We acknowledge financial support from the Deutsche Forschungsgemeinschaft (KU 1531/2-1 and FOR 1162) and from the ESRF, Grenoble, France.

*Present address: Physikalisch-Technische Bundesanstalt, Bundesallee 100, 38116 Braunschweig, Germany.

[1] S. Kera, H. Yamane, and N. Ueno, Prog. Surf. Sci. **84**, 135 (2009).
[2] T. Kataoka, H. Fukagawa, S. Hosoumi, K. Nebashi, K. Sakamoto, and N. Ueno, Chem. Phys. Lett. **451**, 43 (2008).
[3] M. Lackinger and M. Hietschold, Surf. Sci. **520**, L619 (2002).
[4] A. Gerlach, F. Schreiber, S. Sellner, H. Dosch, I. A. Vartanyants, B. C. C. Cowie, T. L. Lee, and J. Zegenhagen, Phys. Rev. B **71**, 205425 (2005).
[5] R. A. J. Woolley, C. P. Martin, G. Miller, V. R. Dhanak, and P. J. Moriarty, Surf. Sci. **601**, 1231 (2007).
[6] Y. Bai, F. Buchner, M. T. Wendahl, I. Kellner, A. Bayer, H.-P. Steinrück, H. Marbach, and J. M. Gottfried, J. Phys. Chem. C **112**, 6087 (2008).
[7] X. Lu, K. W. Hipps, X. D. Wang, and U. Mazur, J. Am. Chem. Soc. **118**, 7197 (1996).
[8] M. Häming, A. Schöll, E. Umbach, and F. Reinert, Phys. Rev. B **85**, 235132, (2012).
[9] I. Kröger, B. Stadtmüller, C. Stadler, J. Ziroff, M. Kochler, A. Stahl, F. Pollinger, T. L. Lee, J. Zegenhagen, F. Reinert, and C. Kumpf, New J. Phys. **12**, 083038 (2010).
[10] C. Stadler, S. Hansen, I. Kröger, C. Kumpf, and E. Umbach, Nat. Phys. **5**, 153 (2009).
[11] C. Stadler, S. Hansen, F. Pollinger, C. Kumpf, E. Umbach, T. L. Lee, and J. Zegenhagen, Phys. Rev. B **74**, 035404 (2006).
[12] M. Häming, C. Scheuermann, A. Schöll, F. Reinert, and E. Umbach, J. Electron Spectrosc. Relat. Phenom. **174**, 59 (2009).
[13] B. Stadtmüller, I. Kröger, F. Reinert, and C. Kumpf, Phys. Rev. B **83**, 085416 (2011).
[14] I. Kröger, B. Stadtmüller, C. Kleimann, P. Rajput, and C. Kumpf, Phys. Rev. B **83**, 195414 (2011).
[15] I. Kröger, B. Stadtmüller, C. Wagner, C. Weiss, R. Temirov, F. S. Tautz, and C. Kumpf, J. Chem. Phys. **135**, 234703 (2011).
[16] J. Zegenhagen, Surf. Sci. Rep. **18**, 199 (1993).
[17] D. P. Woodruff, Prog. Surf. Sci. **57**, 1 (1998).
[18] J. J. Lee, C. J. Fisher, D. P. Woodruff, M. G. Roper, R. G. Jones, and B. C. C. Cowie, Surf. Sci. **494**, 166 (2001).
[19] B. W. Batterman, Rev. Mod. Phys. **36**, 681 (1964).
[20] C. Stadler, S. Hansen, A. Schöll, T.-L. Lee, J. Zegenhagen, C. Kumpf, and E. Umbach, New J. Phys. **9**, 50 (2007).
[21] A. Gerlach, S. Sellner, F. Schreiber, N. Koch, and J. Zegenhagen, Phys. Rev. B **75**, 045401 (2007).
[22] A. Hauschild, K. Karki, B. C. C. Cowie, M. Rohlfing, F. S. Tautz, and M. Sokolowski, Phys. Rev. Lett. **94**, 036106 (2005).
[23] G. Mercurio, E. R. McNellis, I. Martin, S. Hagen, F. Leyssner, S. Soubatch, J. Meyer, M. Wolf, P. Tegeder, F. S. Tautz, and K. Reuter, Phys. Rev. Lett. **104**, 036102 (2010).

[24] J. Stanzel, W. Weigand, L. Kilian, H. L. Meyerheim, C. Kumpf, and E. Umbach, Surf. Sci. **571**, L311 (2004).
[25] N. Koch, A. Gerlach, S. Duhm, H. Glowatzki, G. Heimel, A. Vollmer, Y. Sakamoto, T. Suzuki, J. Zegenhagen, J. P. Rabe, and F. Schreiber, J. Am. Chem. Soc. **130**, 7300 (2008).
[26] J. M. Gottfried and H. Marbach, Z. Phys. Chem. **223**, 53 (2009).
[27] T. Lukasczyk, K. Flechtner, L. R. Merte, N. Jux, F. Maier, J. M. Gottfried, and H. P. Steinrück, J. Phys. Chem. C **111**, 3090 (2007).
[28] K. W. Hipps, X. Lu, X. D. Wang, and U. Mazur, J. Phys. Chem. **100**, 11207 (1996).
[29] X. Lu and K. W. Hipps, J. Phys. Chem. B **101**, 5391 (1997).
[30] S. K. M. Henze, O. Bauer, T. L. Lee, M. Sokolowski, and F. S. Tautz, Surf. Sci. **601**, 1566 (2007).
[31] B. Cordero, V. Gomez, A. E. Platero-Prats, M. Reves, J. Echeverria, E. Cremades, F. Barragan, and S. Alvarez, Dalton Trans. **21**, 2832 (2008).
[32] A. Bondi, J. Phys. Chem. **68**, 441 (1964).
[33] A. Hauschild, R. Temirov, S. Soubatch, O. Bauer, A. Schöll, B. C. C. Cowie, T.-L. Lee, F. S. Tautz, and M. Sokolowski, Phys. Rev. B **81**, 125432 (2010).
[34] M. Chen, X. Feng, L. Zhang, H. Ju, Q. Xu, J. Zhu, J. M. Gottfried, K. Ibrahim, H. Qian, and J. Wang, J. Phys. Chem. C **114**, 9908 (2010).
[35] T. E. Shubina, H. Marbach, K. Flechtner, A. Kretschmann, N. Jux, F. Buchner, H.-P. Steinrück, T. Clark, and J. M. Gottfried, J. Am. Chem. Soc. **129**, 9476 (2007).